*Acta Mineralogica-Petrographica, Szeged 2004, Vol. **45/1**, pp. 101–106*

ACTA
Mineralogica
Petrographica

MINERALOGICAL AND MICROSTRUCTURAL FEATURES OF CHALCEDONY FROM MÁTRA MTS, NORTHERN HUNGARY – A TEM STUDY

VIKTÓRIA KOVÁCS KIS, ISTVÁN DÓDONY

Department of Mineralogy, Eötvös Loránd University, H-1117 Budapest, Pázmány Péter sétány 1/C, Hungary
e-mail: vis@ludens.elte.hu

ABSTRACT

The association and structural relationships of moganite, a recently described silica polymorph, and microcrystalline silica were studied using petrographic microscopy, X-ray powder diffraction, and scanning and transmission electron microscopy. We studied a chalcedony sample, a common fibrous microcrystalline silica variety from Gyöngyössolymos, northern Hungary. Morphological and optical characteristics such as fiber striations and wrinkle banding and the association of mineral phases (quartz, moganite and cristobalite) are reported. Selected-area electron diffraction patterns of twinned domains with periodic and non-periodic twin planes are discussed in relation to moganite and quartz structures.

Key words: microcrystalline silica, quartz, moganite, microstructure, SAED

INTRODUCTION

Silica is one of the most abundant compounds of the Earth's crust and its microcrystalline varieties are widespread in all geologic environments. On the basis of compositional and structural properties, microcrystalline silica includes two main groups (Flörke et al., 1991; Graetsch, 1994): opal and the so-called microcrystalline quartz. Microcrystalline quartz involves chalcedony, quartzine varieties, as well as non-fibrous chert and flint.

Chalcedony is one of the most abundant and studied groups of microcrystalline quartz. In spite of the differences between chalcedony and quartz that have been well known over centuries (Michel-Lévy and Munier-Chalmas, 1892), chalcedony has been regarded to be a quartz variety on the basis of the similar X-ray powder diffraction (XRD) profiles of chalcedony and quartz. In the last decades transmission electron microscopic (TEM) studies revealed the real structural differences between quartz and chalcedony. Besides the distinct quartz reflections, an intense scattering system can be observed perpendicular to {101} quartz planes in selected-area electron diffraction (SAED) patterns of chalcedony samples (Miehe et al., 1984; Graetsch et al., 1987; Wenk et al., 1988; Heaney et al., 1994; Cady et al., 1998; Xu et al., 1998). These reflections are characteristic for chalcedony and they reflect the existence of Brazil-law twinning on a micro-scale.

A new silica polymorph, moganite was reported by Flörke et al. (1976, 1984), and its properties were subsequently detailed in several papers (Miehe and Graetsch, 1992; Heaney and Post, 1992; Kingma and Hemley, 1994; Gíslason et al., 1997; Götze et al., 1998; Parthasarathy et al., 2001; Rodgers and Cressey, 2001; Léger et al., 2001). Structural studies on moganite revealed its close relationship with other microcrystalline silica varieties. The structural data of moganite could be interpreted as if the moganite structure arises from a periodic Brazil-law twinning of quartz, where the twin-related units are the $d_{(101)}$ slabs. Using this concept, microcrystalline silica samples were deconvoluted to quartz and moganite components on the basis of their XRD patterns (Heaney and Post, 1992). The same concept was adopted for the interpretation of TEM results (Heaney et al., 1994; Cady et al., 1998; Xu et al., 1998). However, some problems arose in the interpretation of both SAED and XRD patterns. In calculated XRD patterns the crucial reflections corresponding to moganite spacings are forbidden by symmetry or much less intense than in experimental patterns. Additionally, a {011} continuous scattering system, non-equivalent to the {101} system, is evident in the published SAED patterns (Heaney et al., 1994; Xu et al., 1998). Although these contradictions were mentioned in the above cited papers, the basic concept of the quartz–moganite structural relationship, as described above, is generally accepted.

The formation of microfibrous silica was intensely studied in relation to its microstructure. Based on experimental data, several models were proposed for the silica microstructure, such as a screw dislocation-induced spiral-growth mechanism (Frondel, 1978; Heaney, 1993), or a self-organizational origin of the fibers (Wang and Merino, 1990, 1995; Merino et al., 1995; Heaney and Davis, 1995). Although these deductions are logically correct, Cady et al. (1998) pointed out that they do not yield a satisfactory explanation for the observed planar disorder.

The goals of this paper are to measure microstructural features and to deduce a growth mechanism for a chalcedony sample from northern Hungary. After describing the morphological and optical characteristics of the sample, we present our microstructural observations. We discuss the structural relationships between quartz and moganite comparing previous and our own observations, and give SAED evidence of the moganite and cristobalite content of chalcedony.

Sample and experimental methods

The studied chalcedony sample is a geode from an epithermal vein near Gyöngyössolymos, Mátra Mountains, northern Hungary. The diameter of the geode is 1.5 to 2 cm, and is covered by a thin, dark brown limonitic crust, and with mm-sized euhedral quartz crystals in its core. The fibrous appearance is discernible on the macro-scale; fiber lengths are about 1 cm. The fibers consist of alternating bands of translucent and milky layers perpendicular to the fiber elongations.

Petrographic microscopy was performed on uncovered thin sections before and after etching with a 40% HF : H_2O solution for 10 s (Takács, 1982). The etched surface was also examined with a Hitachi S-2460 scanning electron microscope, operating at 30 kV.

XRD patterns were obtained using a Philips PW 1710 diffractometer operating at 45 kV and 35 mA with CuK radiation in the 12° to 70° 2θ range. For comparison we used an XRD pattern of a macro-quartz sample (from Telkibánya, Hungary).

Sample fragments for TEM study were crushed under ethanol and deposited onto Cu grids covered by holey-carbon supporting films. SAED patterns were obtained using a JEOL 100U TEM operating at 100 kV. We simulated XRD and SAED patterns using the Cerius^2 3.5 software (Molecular Simulations Institute, Inc.) and structural data listed for quartz and moganite by Heaney (1994) and Miehe and Graetsch (1992), respectively.

Results

Morphological and optical properties

The coarse inner surface of the geode crust yields nucleation centers for the fiber growth. Initiating fibers produce parabolic bundles that grow inward the geode. As the bundles reach a certain width, they join other bundles that are growing in adjacent sectors (Fig. 1). These sectors are well recognizable under cross-polarized light because their extinctions do not occur simultaneously. The fibers are optically length-fast. Based on textural properties, the sample can be classified as consisting of "parabolic, fibrous wall-lining bundles" in the nomenclature of Flörke et al. (1991).

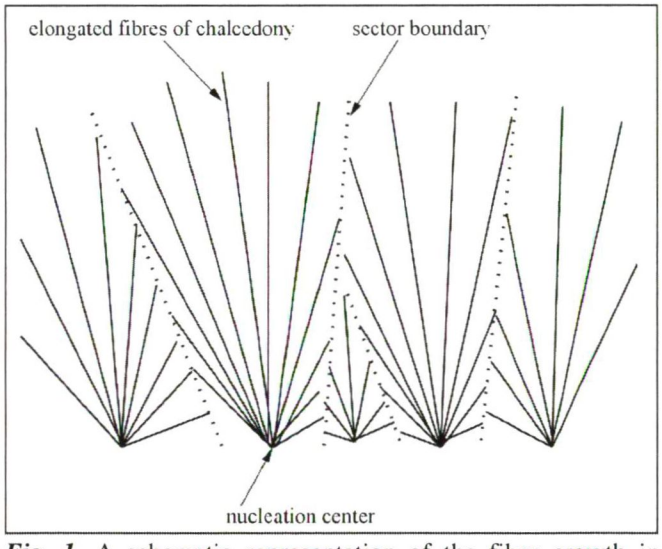

Fig. 1. A schematic representation of the fiber growth in parabolic fibrous wall-lining chalcedony (after Flörke et al. 1991). The dotted line is the boundary between the sectors which form by the contact of the parabolic fiber bundles.

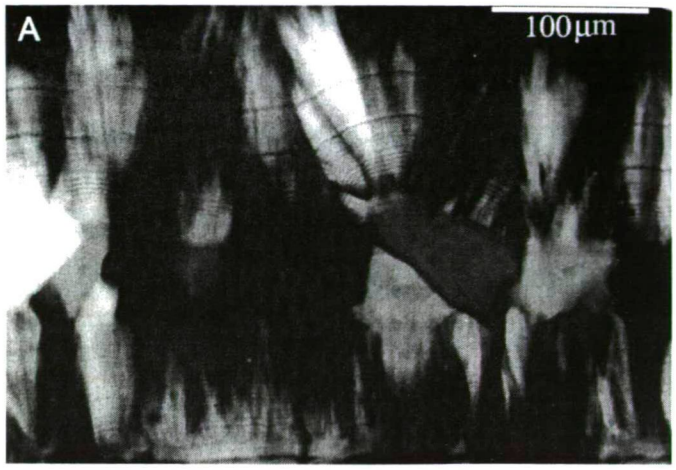

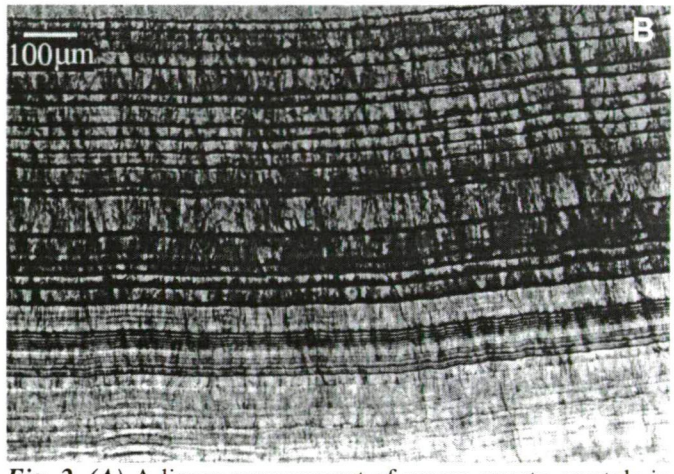

Fig. 2. (A) A linear arrangement of macro-quartz crystals in the chalcedony forms new nucleation centers. Cross-polarized light. ***(B)*** Changing periodicity of fiber striation perpendicular to the elongation direction. The periodicity varies between 5 μm and 50 μm.

Fig. 2 shows several features of chalcedony that are observable in a petrographic microscope: nucleation characteristics, fiber striations and wrinkle banding. The fibrous texture is assumed to be due to the spontaneous fingering of morphologically unstable crystallization fronts (Wang and Merino, 1995). The morphological instability is promoted by the high growth rate, high supersaturation and presumably the presence of certain cations such as Al^{3+}, and impeded by solubility and surface tension. Varying crystallization conditions may upset the temporal equilibrium between these factors, causing precipitation of non-fibrous microcrystalline quartz layers. These quartz crystals that break the fiber continuity through several sectors (Fig. 2A) serve as new nucleation centers for chalcedony fibers, when the fibrous morphology is favored again.

Striations perpendicular to the fibers are visible in both polarized and ordinary light (Fig. 2). The striations are enhanced on etched surfaces (Fig. 2B and Fig. 3); they may be curved where the fiber bundles are still distinguishable (Fig. 2A), and straight where the individual bundles are not recognizable (Fig. 2B). The striations break at the sector

boundaries. Their spacing may be uniform over short distances, but generally varies within a few orders of magnitude and is getting finer towards the crust of the geode.

The surface morphology after etching is illustrated by the SEM photograph in Fig. 3. The striations appear similar as under the petrographic microscope, but more detail is revealed about the fibrous microstructure. The thickness of individual striations varies in the range of 5 to 30 μm, and is getting finer towards the crust of the geode.

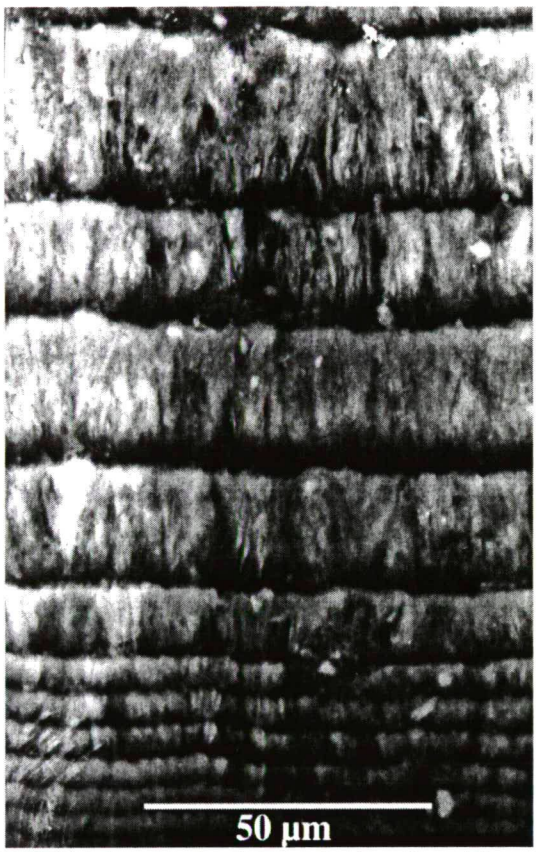

Fig. 3. SEM micrograph of the etched surface. The crust of the geode is downward. Note the surface morphology formed by the selective solution on etching and the changing spacing of the striations towards the core. The fine structure of the fibers between the individual striations is also observable.

The striations are characteristic of wall-lining chalcedonies. They are considered to be internal boundaries between zones of different optical densities (Frondel, 1978, 1982) that are supposed to be related to the changing amount of molecular water along the fiber length. The sharp changes in the surface morphology as revealed by SEM images are attributable to differences in the water content; stripes that have higher water concentrations etch more easily than regions with low water contents. Similar striations were observed in opal-C and non-crystalline hyalite as well (Graetsch, 1994).

As observed by Michel-Lévy and Munier-Chalmas (1892), chalcedony shows oscillatory extinction bands in cross-polarized light (Fig. 2A). That is, extinction along a fiber does not occur simultaneously, but sections alternate that are in and out of extinction. These sections neither form a continuous zone, nor are they perpendicular to the fiber elongation; thus, extinction bands have a zigzag appearance. This phenomenon is called "wrinkle banding" or "Runzelbanderung", and was observed in whisker crystals of metals as well (Frondel, 1978). Wrinkle banding arises from the twisting of the fiber around its axis. The twist period, which depends on the crystallisation temperature, ordinarily is uniform along the fiber length, but tends to increase with increasing fiber thickness (Frondel, 1978).

The zigzag character of the extinction bands is caused mainly by a slight angular divergence or slight displacement along the fiber length of the adjacent fiber bundles (Frondel, 1978). In case of large displacements, the extinction has a mosaic-like appearance as it was observed on the Gyöngyössolymos sample.

XRD measurements

The XRD pattern of the sample is dominated by the reflections of quartz. Anomalies with respect to quartz appear in reflections of minor intensities. Fig. 4 shows two selected regions of the experimental XRD patterns of the measured chalcedony and the reference macro-quartz samples, together with the simulated XRD profile of moganite. The chalcedony pattern deviates from that of quartz at the places of moganite peaks (arrowed). The weak reflection at about $2\theta = 19.4°$ is interpretable as the 100 reflection of hexagonal tridymite, or 102 and $10\bar{2}$ of moganite; however, these moganite reflections are forbidden by symmetry. Although the calculated positions of 011 and $0\bar{1}1$ reflections of moganite ($2\theta = 20°$) are a little off from the observed 19.4° 2θ value, the poor statistics allows the interpretation of this reflection as moganite.

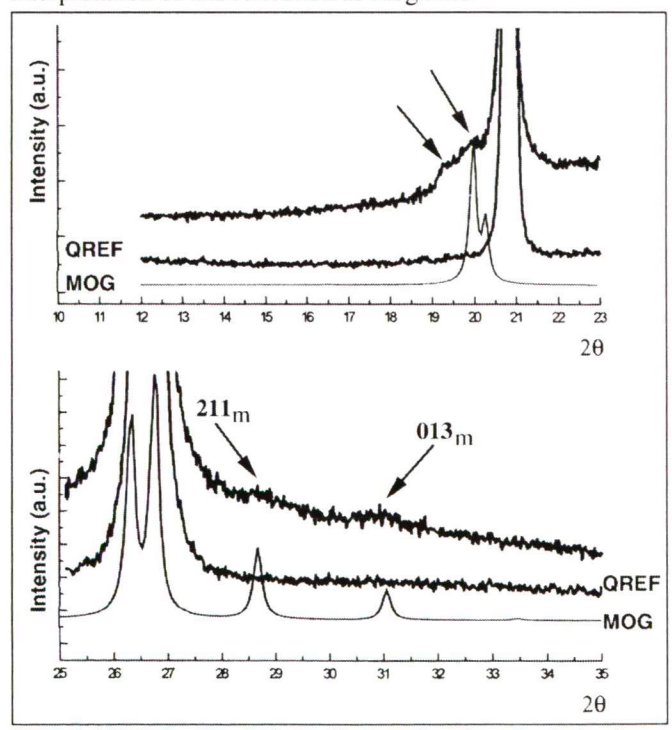

Fig. 4. XRD patterns of the Gyöngyössolymos chalcedony, the reference macrocrystalline quartz from Telkibánya and the simulated profile of moganite. The arrows show the reflections that distinguish chalcedony from quartz. Two of them coincide with moganite 211 and 013 reflections. Note the peak broadening in the case of the chalcedony; the FWHM values exceed that of macro-quartz by approximately 30 %.

The full width at half maximum (FWHM) value numerically characterizes the peak profile. The average crystallite size is one of the most significant parameters affecting the FWHM. Differences in the FWHM values between chalcedony and macro-quartz illustrate the microcrystalline character of chalcedony: the larger the FWHM value, the smaller the mean crystallite size ($FWHM(100)_{Ch}$ = 0.244, $FWHM(011)_{Ch}$ = 0.208; $FWHM(100)_{Q}$ = 0.172, $FWHM(011)_{Q}$ = 0.159).

Microstructure

On a submicroscopic scale, grains of the main quartz phase consist of domains. Most of these domains have the structure of quartz (Fig. 5), but several of them show disorder or superstructures. SAED patterns illustrate well the microstructural variability of chalcedony.

The presence of twinning are observable viewing down <$\bar{1}\bar{2}$1> or <$\bar{2}\bar{1}$1>, parallel to the possible composition planes. Calculated diffraction patterns confirm the expectations that the <$\bar{1}\bar{2}$1> and <$\bar{2}\bar{1}$1> patterns are the same by geometry, but differ in their intensity distributions. However, in practice it is rather hard to differentiate which one is the actually observed projection, and indexing of the diffraction patterns in these orientations is ambiguous. In this paper we follow the notation of Miehe et al. (1984).

A Brazil-law twin boundary in quartz produces one $d_{(101)}$ = 6.68 Å thick moganite slab. A streaking perpendicular to the composition planes appears in SAED patterns, the intensity of which is proportional to the density of twinning. The intensity distribution along a streak characterizes the order-disorder nature of the twinned parts. In the case of a periodical {101} twin system, a superlattice can be expected with a periodicity of $n \cdot d_{(101)}$ (where $d_{(101)}$ = 3.34 Å and n is an integer). The moganite structure represents the possible highest twin density (n = 2).

[$\bar{1}\bar{2}$1] SAED patterns in Fig. 5 show the effects of one set of the possible composition planes. Weak but sharp reflections occur halfway between the intense quartz reflections along [101]* and [$\bar{1}$11]*, showing the characteristic 6.68 Å spacing (n = 2) of moganite (Fig. 5A, B). The sharpness of these halving reflections is proportional to the average thickness of moganite domains perpendicular to the twin planes. The intensity distributions along the [101]* and [$\bar{1}$11]* axes vary with the distances between neighboring twin planes and their ordering. The intensity distribution of streaking along these directions of quartz is a measure of the density distribution of non-periodic twin boundaries (Fig. 5A). In Fig. 5C the rows of sharp extra reflections are parallel to the [012]* direction of quartz.

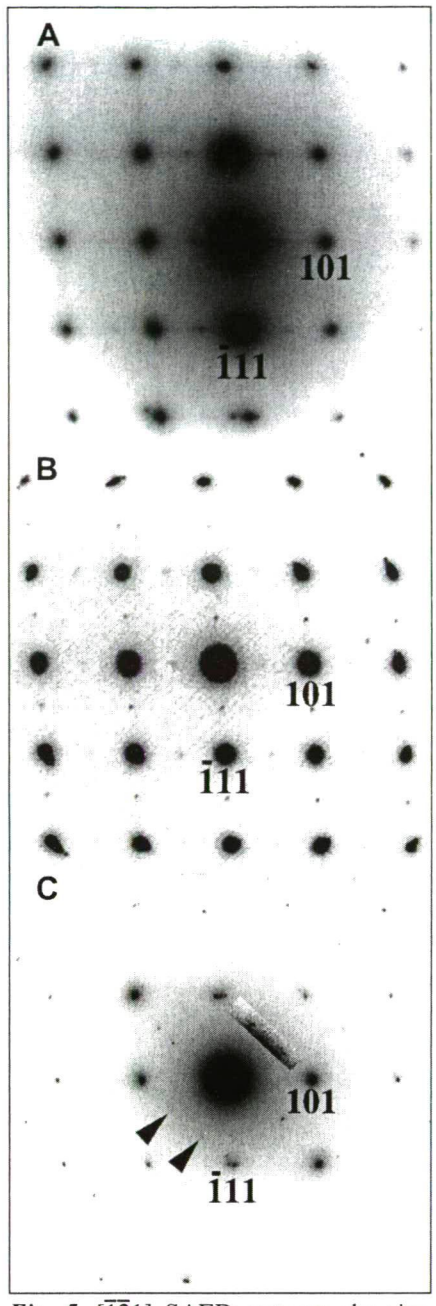

Fig. 5. [$\bar{1}\bar{2}$1] SAED patterns showing deviations from the ideal quartz pattern. (a) Both streaking and lenticular-shaped reflections are superimposed parallel to [101]* and [$\bar{1}$11]* axes. (b) Sharp superlattice reflections are detectable between the intense quartz reflections. (c) Neither streaking nor sharp reflections, but a pair of vague extra spots (marked with arrowheads) are present parallel to the [012]* quartz direction.

Similar to the [$\bar{1}\bar{2}$1] projections, there are several indexing possibilities for the <$\bar{1}\bar{1}$1> and <10$\bar{1}$> SAED patterns. These projections contain a pair of non-equivalent <101>* and <011>* directions. Disregarding disparities originating from the handedness, all <$\bar{1}\bar{1}$1> and <10$\bar{1}$> patterns have to be identical; there should not be any difference between intensity distributions in these projections, even taking into account multiple scattering. At the same twin densities the diffracted intensity distributions along the <101>* and <011>* directions must be the same. However, owing to the twin-related diffraction features, the intensity distributions in experimental <111> and <10$\bar{1}$> SAED patterns are not the same.

The non-equivalent [101]* and [011]* directions are different in Fig. 6A: streaking occurs along [101]* only, indicating random twinning only in this direction. On the other hand, parallel to [011]* there are sharp intensity maxima at $h \pm 1/2$, k, $l \pm 1/2$. The continuous scattering along [101]* and [011]*, the two non-equivalent directions, is practically the same in Fig. 6B.

SAED patterns presented in Fig. 7 represent two other silica components of chalcedony, moganite and cristobalite. Regarding solely the geometry of Fig. 7A, it corresponds to a [100] moganite pattern, but the group of strong reflections indicates a high proportion of [$\bar{1}$10]-oriented quartz in the selected area. The orientations of quartz and moganite components correspond to the orientation and symmetry relationships as identified by Miehe and Graetsch (1992). Fig. 7B can be interpreted as resulting from polycrystalline cristobalite. Most crystallites within the selected region are oriented with their [111] parallel to the electron beam.

Discussion

We interpret morphological and textural inhomogeneities as evidences for fluctuations in conditions during crystallization. Interlayered macro-quartz bands perpendicular to fibers, periodic oscillations of the thickness of striations over several orders of magnitude imply cycles during the precipitation of chalcedony. The concentration of silica in the parent solution and the proportion of water incorporated within the precipitate depend on the parameters of fluctuating conditions (T, pH and P). The observed wrinkle banding with decreasing periodicity towards the core of the geode may be considered as a result of the oscillating temperature during crystal growth (Frondel, 1978).

The cyclic crystallization affects the crystal structure as well (Heaney and Davis, 1995). SAED patterns prove that many silica polymorphs are present in the sample. Diffraction patterns in Fig. 5, 6 are indexed as produced by quartz. Since the structures of quartz and moganite are closely related, an examination of these diffraction patterns considering moganite structure is also warranted. According to the symmetry of moganite, the main directions in Fig. 5, 6 will be $[101]^*_{mog}$ and $[2\bar{1}\bar{1}]^*_{mog}$, and $[101]^*_{mog}$ and $[112]^*_{mog}$, respectively. The $[101]^*_{mog}$ axis coincides with $[101]^*_{quartz}$. Reflections at 6.68 Å correspond to $d_{(101)}$ of moganite, which is forbidden by the I2/a symmetry. Calculated $[\bar{1}\bar{1}1]$ and $[\bar{1}31]$ SAED patterns for moganite show 6.68 Å reflections at specimen thicknesses greater than 100 and 120 Å, respectively. That is, the presence of the halfway reflections parallel to $[101]^*_{quartz}$ may be interpreted as a proof of periodic Brazil-law twinning (Heaney et al., 1994; Cady et al., 1998; Xu et al., 1998). However, another explanation for the presence of halfway reflections was given by Heaney et al. (1994); this interpretation does not require a moganite content. In SAED patterns containing streaks nearly perpendicular to the imaged reciprocal plane, the streaks appear as sharp reflections at the intersections of the streaks and the reciprocal plane. In the present study the halving reflections in the SAED patterns likely appear because of the presence of moganite, since a quartz-moganite association is also indicated by the XRD patterns.

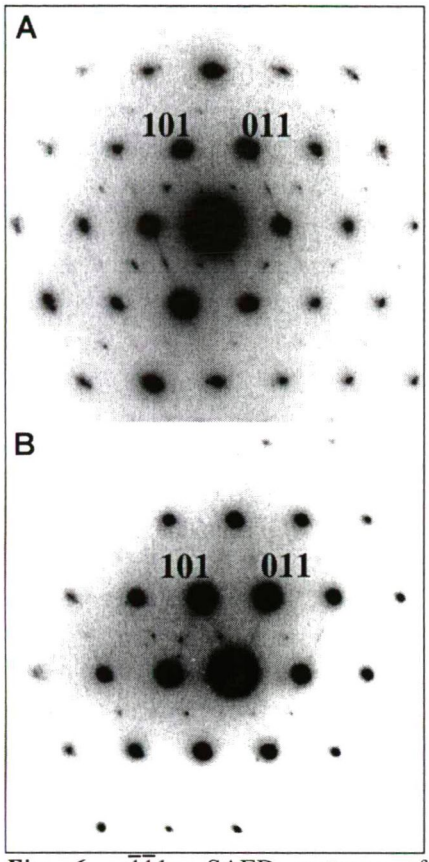

Fig. 6. <$\bar{1}\bar{1}$1> SAED patterns of chalcedony. Note the difference between the two patterns along their [101]* directions. Pattern ***(A)*** shows only sharp extra reflections, the diffuse streak is absent.

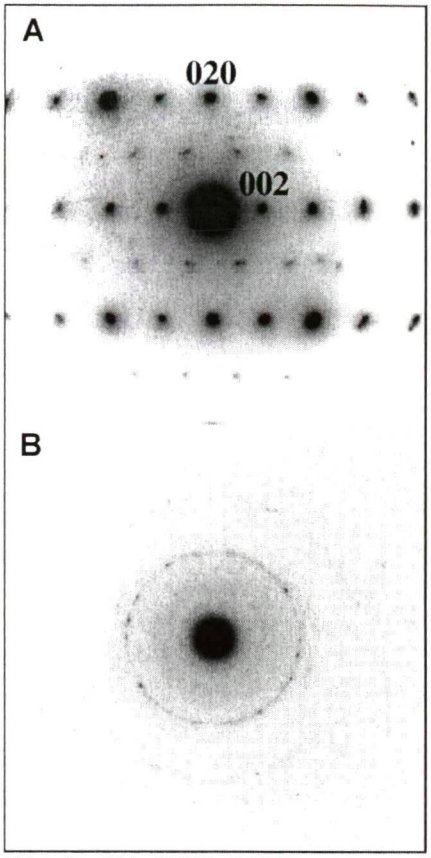

Fig. 7. (A) [100] SAED pattern of moganite ***(B)*** Ring-like [111] SAED pattern of polycrystalline cristobalite.

However, periodic Brazil-law twinning of quartz cannot satisfactorily explain the <$\bar{1}\bar{1}$1> and <10$\bar{1}$> SAED patterns, since high-resolution images (Xu et al., 1998, and our unpublished images) show mainly non-periodic twinning. According to these observations, the halfway reflections parallel to quartz <101>* are accompanied by streaks (Fig. 5A, 6B), whereas there is no streaking in many SAED patterns (Fig. 5B, 6A). Additionally, in Fig. 5B extra reflections are present parallel to both [101]* and $[\bar{1}11]$* of quartz, which is inconsistent with a moganite structure.

According to McLaren and Pitkethly (1982), the possible composition planes of Brazil-law twins are {101} and {011}. The application of Miehe conventions for quartz-moganite indexing is consistent with the results of Wang and Merino (1990), who deduced that the {101} planes are energetically favored among the possible composition planes of Brazil-law twinning. The high probability of twin planes occurring along {101} planes results in moganite in the case of the highest twin plane density (n = 2), whereas in the non-favored <011> directions the lower twin density produces streaks in SAED patterns. In Fig. 6A the streaks are parallel to the <011>*, indicating non-periodic twin boundaries; the halfway reflections are along one of the <101>* axes at $h\pm1/2$, k, $l\pm1/2$, suggesting periodic twin boundaries over a larger area that is considered moganite intergrown with the quartz host.

Fig. 5C is a similar SAED pattern to that published by Miehe et al. (1984) and Heaney et al. (1994), with the difference that it does not show streaks, but contains only sharp extra reflections. Following the interpretation of Heaney et al. (1994), these reflections are the intersections of

an <011> streak system with the reciprocal plane defined by the [101]* and [$\bar{1}$11]* vectors.

The XRD measurements suggested the presence of moganite; this result was confirmed by SAED. Fig. 7A is an [011] diffraction pattern of moganite. The sharp reflections indicate ordered submicrometer-sized moganite domains.

Conclusions

The main constituent of chalcedony is quartz; besides it other silica polymorphs: cristobalite (and presumably domains of tridymite-like stacking) and moganite were identified in the studied Gyöngyössolymos sample. To our knowledge, this is the first evidence for a moganite occurrence in Hungary. The minor constituents of chalcedony, moganite and cristobalite, can be detected and measured only by TEM. The quartz domains are twin-related (Brazil-law), where the twin planes can be ordered and may occur periodically or non-periodically. Some superstructure types for chalcedony which were observed in the Göngyössolymos sample are reported for the first time.

Acknowledgements

The authors are grateful to Tibor Nagy for providing the studied sample and to Mária Tóth (Research Laboratory of Geochemistry) and András Falus (Semmelweis University) for the use of XRD and SEM facilities, respectively. We thank Tibor Németh for the XRD measurements, Miklós Pintér for the SEM photograph, and Lívia Rudnyánszky for technical aid.

References

Cady, S. L., Wenk, H. R., Sintubin, M. (1998): Microfibrous quartz varieties: characterization by quantitative X-ray texture analysis and transmission electron microscopy. Contrib. Min. Petr., **130**, 320–335.

Flörke, O. W., Jones, J. B., Schmincke, H. U. (1976): A new microcrystalline silica from Gran Canaria. Zeit. Krist., **143**, 156–165.

Flörke, O. W., Flörke, U., Giese, U. (1984): Moganite: a new microcrystalline silica mineral. N. Jb. Mineral. Abh., **149**, 325–336.

Flörke, O. W., Graetsch, H., Martin, B., Röller, K., Wirth, R. (1991): Nomenclature of micro- and non-crystalline silica minerals based on structure and microstructure. N. Jb. Mineral. Abh., **163**, 19–42.

Frondel, C. (1978): Characters of quartz fibers. Am. Min., **63**, 17-27.

Frondel, C. (1982): Structural hydroxyl in chalcedony. Am. Min., **67**, 1248–1257.

Gíslason, S. R., Heaney, P. J., Oelkers, E. H., Schott, J. (1997): Kinetic and thermodynamic properties of moganite a novel silica polymorph. Geochim. et Cosmochim. Acta., **61**, 1193–1204.

Götze, J., Nasdala, L., Kleeberg, L., Wenzel, M. (1998): Occurrence and distribution of "moganite" in agate/chalcedony: a combined micro-Raman, Rietveld, and cathodluminescence study. Contrib. Min. Petr., **133**, 96–105.

Graetsch, H. (1994): Structural characteristics of opaline and microcrystalline silica minerals. Rev. in Min., **29**, 209–232.

Graetsch, H., Flörke, O.W., Miehe, G. (1987): Structural defects in microcrystalline silica. Phys. Chem. Miner., **14**, 249–257.

Heaney, P. J. (1993): A proposed mechanism for the growth of chalcedony. Contrib. Min. Petr., **115**, 66–74.

Heaney, P. J. (1994): Structure and chemistry of the low-pressure silica polymorphs. Rev. in Min., **29**, 1–122.

Heaney, P. J., Davis, A. M. (1995): Observation of self-organised textures in agates. Science, 269, 1562–1565.

Heaney, P. J., Post, J. E. (1992): The widespread distribution of a novel silica polymorph in microcrystalline quartz varieties. Science, **255**, 441–443.

Heaney, P. J., Veblen, D. R., Post, J. E. (1994): Structural disparities between chalcedony and macrocrystalline quartz. Am. Min., **79**, 452–460.

Kingma, K. J., Hemley, R. J. (1994): Raman spectroscopic study of microcrystalline silica. Am. Min., **79**, 269–273.

Léger, J-M., Haines, J., Chateau, C. (2001): The high-pressure behaviour of the "moganite" polymorph of SiO_2. Eur. J. Miner. **13**, 351–359.

McLaren, A. C., Pitkethly, D. R. (1982): The twinning microstructure and growth of amethyst quartz. Phys. Chem. Miner. **8**. 128–135.

Merino, E., Wang, Y., Deloule, Ä. (1995): Genesis of agates in flood basalts: twisting of chalcedony fibers and trace element geochemistry. Am. J. Sci., **295**, 1156–1176.

Michel-Lévy, A., Munier-Chalmas, C. P. E. (1892): Mémoire sur diverses formes affectées par le réseaux élémentaire du quartz. Bull. Soc. Mineral. Fr., **15**, 159–190. (in French)

Miehe, G., Graetsch, H. (1992): Crystal structure of moganite: a new structure type for silica. Eur. J. Miner., **4**, 693–706.

Miehe, G., Graetsch, H., Flörke, O. W. (1984): Crystal structure and growth fabric of length-fast chalcedony. Phys. Chem. Miner., **10**, 197–199.

Parthasarathy, G., Kunwar, A. C., Srinivasan, R. (2001): Occurrence of moganite-rich chalcedony in Deccan flood basalts, Killari, Maharashtra, India. Eur. J. Miner., **13**, 127–134.

Rodgers, K. A., Cressey, G. (2001): The occurrence, detection and significance of moganite (SiO_2) among some silica sinters. Min. Mag., **65**(2), 157–167.

Takács, J. (1982): Mineralogy of opal. PhD thesis. Manuscript. MTA GKL, Budapest, 124 pp. (in Hungarian)

Wang, Y., Merino, E. (1990): Self-organizational origin of agates: Banding, fiber twisting, composition, and dynamic crystallisation model. Geochim. et Cosmochim. Acta, **54**, 1627–1638.

Wang, Y., Merino, E. (1995): Origin of fibrosity and banding in agates from flood basalts. Am. J. Sci., **295**, 49–77.

Wenk, H. R., Shaffer, S. J., Van Tendeloo, G. (1988): Planar defects in low temperature quartz. Phys. Stat. Sol. A., **107**, 799–805.

Xu, H., Buseck, P. R., Luo, G. (1998): HRTEM investigation of microstructures in length slow chalcedony. Am. Min., **83**, 542–545.